Predicting the effect on pulse wave reflection of different endovascular repair techniques in abdominal aortic aneurysm using 1D patient-specific models

M. E. Casciaro, M. A. Alfonso, D. Craiem, J. M. Alsac, S. El-Batti & R. L. Armentano

Health and Technology

ISSN 2190-7188

Health Technol.
DOI 10.1007/s12553-016-0140-8

Springer

Health Technol.
DOI 10.1007/s12553-016-0140-8

ORIGINAL PAPER

Predicting the effect on pulse wave reflection of different endovascular repair techniques in abdominal aortic aneurysm using 1D patient-specific models

M. E. Casciaro[1] · M. A. Alfonso[4] · D. Craiem[1,2,3] · J. M. Alsac[2,3] · S. El-Batti[2,3] · R. L. Armentano[1,4]

Received: 30 June 2016 / Accepted: 16 September 2016

Abstract Abdominal aortic aneurysm (AAA) is a pathological dilation of the abdominal aorta, generally distal to the renal arteries. In relation to this, minimally invasive endovascular aortic repair has become a common technique, and great efforts have been made to characterize surgical outcome in terms of endograft displacement, leakages, aneurysm sac enlargement or other post-operative complication. Recently, two novel devices (AFX and Nellix sealing device) were developed to surpass these complications, but there is no work accounting for the effects they may have on the pressure waveform. In this study, we address the problem of generating a patient-specific 1D model of an aortic aneurysm, and compute the impact that these devices can have on pressure, in terms of wave reflection. As a result, we found both endovascular repair devices decrease the reflected wave transient time by one order of magnitude, and that the Nellix device shows increased reflected wave amplitude at proximal abdominal aorta and at renal artery level compared to AFX (33 % and 75 % increase in amplitude ratio compared to a non-diseased aorta, respectively). Due to the importance that pressure at renal site and pulse waveform have on the overall cardiovascular physiology, the validity of these results should be carefully studied in order to develop a patient-specific tool for medical planning of interventions.

Keywords Abdominal aortic aneurysm · Endovascular aortic repair · Patient-specific 1D model · Pulse wave reflection

This article is part of the Topical Collection on *Health and Technology in Latin America*

✉ M. E. Casciaro
mecasciaro@gmail.com

[1] Instituto de Medicina Traslacional, Trasplante y Bioingeniería (IMeTTyB), Universidad Favaloro-CONICET, Solís 453, C1078AAI Buenos Aires, Argentina

[2] Service de Chirurgie Cardiaque et Vasculaire, Hôpital Européen Georges Pompidou, Paris, France

[3] INSERM U970, Paris, France

[4] Grupo de Investigación y Desarrollo en Bioingeniería (GIBIO), Universidad Tecnológica Nacional, Buenos Aires, Argentina

1 Introduction

Abdominal aortic aneurysm (AAA) is a pathological dilation of the abdominal aorta, generally distal to the renal arteries. Nowadays, minimally invasive Endo Vascular Aortic Repair (EVAR) has become a more common technique than open surgery [1]. In this direction, two modern AAA EVAR devices can be mentioned: the AFX (Endologix, Irvine, Calif) commercially available since 2011, and Nellix (Endologix, Irvine, Calif), developed in 2011 to surpass many of the complications of endovascular aortic aneurysm repair that arises from inadequate isolation of the diseased aortic wall from pressurized blood flow. The AFX device [2] consists mainly on a single-body bifurcated graft design that rests on the native aortoiliac bifurcation, giving anatomical fixation and reducing type I endoleaks. On the other hand, the Nellix device [3] consists of polyurethane endobags that surround two balloon-expandable stents. Stability of the aneurysm sac is achieved by completely filling the endobags with a polymer that cures at body temperature.

Despite the efforts to characterize the outcome of these novel techniques in terms of endograft displacement, leakages, aneurysm sac enlargement or other post-operative complications [4–9], there is no work accounting for the effects these endoprostheses may have on the Pressure Waveform (PWF). This becomes relevant as PWF is being ascribed an increasingly important role in the evaluation of cardiovascular

Published online: 01 October 2016

risk [10]. Although the effect that different EVAR devices may have on PWF is hard to measure in vivo, simple one-dimensional (1D) models could contribute to this understanding at a reasonable computational cost. Comparisons against in vivo and in vitro data have shown the ability of the nonlinear 1D equations of blood flow in compliant vessels to capture the main features of pressure and flow waveforms in large arteries [11, 12], and hence it was suggested that 1D models could provide a suitable tool for patient-specific medical planning of interventions [13].

To the best of our knowledge, the effect of the AFX and Nellix endoprothesis on central PWF has not been addressed before, despite some attention has been given to the effects of non-treated AAAs [14] and more traditional EVAR techniques [15] using patented software. Therefore, the aim of this research was to study the effect that this novel AAA repair techniques may have on the PWF. To address the problem, we assessed a patient-specific geometry of a clinically relevant AAA from a computer tomography (CT) scan and used this three-dimensional information to construct an axisymmetrical 1D model of the abdominal aorta, that could acquaint for bifurcating flows as well as fluid-wall interactions [16]. Simulations were performed in four different situations: normal (non-dilated) aorta, aortic aneurysm, AFX repaired aneurysm and Nellix repaired aneurism. Data were analysed in terms of pressure wave reflection using realistic values for elastic modulus and aortic geometry.

2 Materials and methods

The diseased aorta of a 76 y.o. male patient (66 kg, 1.71 m height, non-diabetic, non-hypercholesteraemic and with treated HTA) was carried out using 64-slice CT contrast enhanced angiography scan images at the Cardiovascular Surgery Unit of the Hôpital Européen Georges-Pompidou (France). The scanner used was a Lightspeed VCT (GE Health care, Milwaukee, Wisconsin, USA). Matrix size was 512 × 512 and axial slice distance was 1 mm. The patient had undergone infrarenal AAA repair with Nellix endoprothesis in November 2013, and signed an approved informed consent before the surgery. The retrospective analysis of personal health data of study subjects had the authorization of the CNIL (Commission Nationale de l'Informatique et des Libertes) and was in accordance with the declaration of Helsinki.

2.1 Aortic segmentation

A geometric deformable model (GDM) originally used to quantify aneurysm lumen volume [9] was used to perform the aortic segmentation process. Briefly, the GDM segmentation emulates a virtual elastic balloon that inflates inside a region of interest. The GDM initial shape is a balloon composed by vertexes connected with springs forming triangular faces. Intensities inside this initial balloon (quantified in Hounsfield units) are used to compute mean and standard deviation values and to set the deformable model parameters. The position of each vertex is dynamically calculated using internal and external forces. Internal forces consist of stretching, bending and dissipative forces, while an external inflation force pushes each vertex of the mesh perpendicularly to the surface. These forces can make the mesh to locally expand or compress, morphing the GDM from a sphere into its final shape. Dynamic face subdivision/collapsing allow maintaining an average mesh resolution set by the operator. More details about this GDM can be found elsewhere [9].

For our purpose, the balloon was positioned inside the polymer filled Nellix endobag after virtual stents removal achieved by a standard region growing algorithm, starting in a user-selected pixel belonging to the stent. All connected neighbours intensities were replaced by the mean intensity value. The GDM was allowed to grow from the uppermost region of the aorta inside the CT field of view (almost at coronary sinus level) to the left and right common iliac bifurcations.

2.2 Patient-specific 1D model extraction

With the segmented aortic shape a 1D model was obtained by computing the mesh centreline and calculating the radius of the cross-sectional area (CSA) at each centreline point. As a result, diameter vs centreline distance function was obtained in steps of 0.5 mm (Fig. 1).

2.3 Aortic regions subdivision

The one dimensional aortic model was subdivided in four regions:

- **Proximal aorta (non-diseased):** the aorta proximal to the heart from coronary sinus level to the right renal artery ostium. This region includes the celiac trunk, mesenteric artery and left renal artery. The beginning of this region is set as the model input region.
- **Post renal aortic segment (non-diseased to diseased transition):** this region goes between the right renal artery to the beginning of the aneurysm (aneurysm neck).
- **Aneurism region (diseased):** this region goes between the beginning of the aneurysm at the abdominal aorta to the end of dilated portions of the common iliac arteries. It includes the aneurysm neck, body and aortic bifurcation.
- **Iliac region (non-diseased):** these regions (left and right) go from the end of the dilated portions of the common iliac arteries (aneurysm end) to the common iliac bifurcation in external and internal iliac arteries.

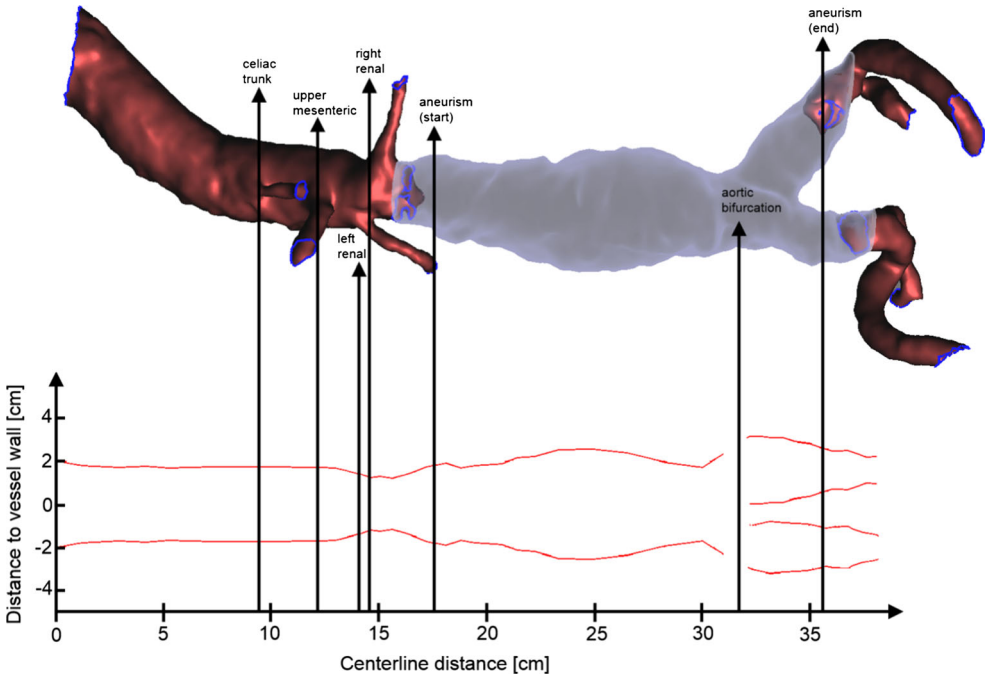

Fig. 1 Axisymmetrical 1D model of the patient aneurysm. Different aortic regions are indicated with arrows. Red portion of the aorta indicates regions with no EVAR (Nellix) presence in the real TC study, while grey region indicates the opposite

2.4 One-dimensional flow model

The 1D axisymmetrical model can be divided in two main constituents: an incompressible Newtonian fluid model for blood and an incompressible hyper elastic solid model for the arterial wall. Fluid dynamics equations are solved numerically by a finite element method, with a penalization method to acquaint for the incompressibility conditions. For the fluid-solid interaction, a partitioned method with strong coupling and Arbitrary Lagrangian-Eulerian (ALE) formulation is used, that can take into account the movement of the fluid boundaries. Details about the model can be found elsewhere [16, 17]. To further simplify the simulations using this model, conditions of no-reflection are set in the iliac arteries (model output) and at the proximal abdominal aorta (model input). Moreover, no angular considerations were considered in the model (i.e. a 0° angle was considered at the aortoiliac bifurcation).

2.5 Model parameters

According to the age and sex of the patient, the elastic modulus of the non-diseased part of the aorta (E_{nd}) and aortic aneurysm (E_{an}) were selected as 4.10^5 and 6.10^5 Pa, respectively [18, 19]. An aortic thickness of 2 mm and 2.5 mm [20] was considered for the non-diseased and aneurysmal regions respectively. A linear transition between non diseased and diseased parameters was considered for the post renal aortic segment region.

The elastic moduli of the Nellix and AFX stents were estimated using a model for Nitinol stents [21] replacing the Nitinol's wire elastic modulus with that of Cromium Cobalt (CrCo) alloys [22]. The aforementioned model computes stent elastic modulus as:

$$Es = \frac{3En^3d^4}{8\pi^6r^4}$$

Where E is the CrCo wire Young Modulus (E = 198 MPa), n is the number of semicircles that form one level of stent cells (n = 12 for both Nellix and AFX stents), d is the wire diameter (d = 1 mm for both Nellix and AFX), and r is the stent nominal radius (r = 5 mm and 12.5 mm for Nellix and AFX stents respectively). This gives a value of E_s = 200 MPa and 5 MPa for Nellix and AFX stents respectively.

2.6 Simulations

Simulations for 1D flow were performed in 4 different models (Fig. 2):

1. Bare aneurysm.
2. Nellix endoprothesis repair.
3. AFX endoprothesis repair.
4. Normal aorta.

Parameters for the four simulations are presented in Table 1. Data for stent thickness and nominal diameters were obtained from literature [4, 23].

In order to isolate the effects that each model has on PWF, no other reflective phenomena (such as peripheral resistance or bifurcation angles) were considered in the simulations. For

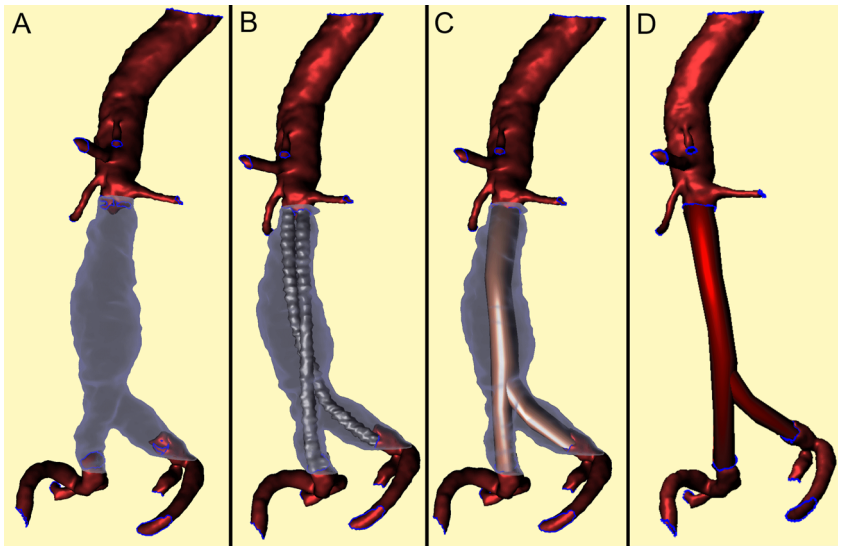

Fig. 2 **a** Aneurysm model, **b** Nellix EVAR device, **c** AFX EVAR device, **d** Normal aorta model

each model, a pressure impulse was introduced (40 mmHg amplitude lasting 5.10^{-3} s), and the maximum reflected pressure was recorded at the input site and renal level. Simulation time interval was chosen as 0.1 s.

3 Results

Figure 3 shows the PWF of the 4 different simulations. Table 2 depicts the reflected wave amplitude ratio (calculated as the ratio between reflected wave amplitude and incident wave amplitude), and the reflection time (computed as the elapsed time between the input wave and the reflected wave reaching the same site).

It can be seen that the bare aneurysm shows the less amplitude reflection both at renal level and at input site, while reflection times are similar to those obtained for the normal aorta. From Fig. 3, we can assume that for both these simulations, the origin of most of the reflected wave is due to the aortoiliac bifurcation. On the other hand, both EVAR devices show one order of magnitude smaller reflection times, indicating that most of the reflected wave comes from: impedance uncoupling due to abrupt elastic modulus changes for both AFX and Nellix device, and additional impedance uncoupling in the latter due to early flow bifurcation. This last observation can be further supported by the greater reflected amplitude that the Nellix device shows at both renal level and input size when compared to AFX device.

4 Discussion

Pulse waveform analysis in the four models show different behaviours of the simulated pressure pulse in terms of reflected amplitude and time. In agreement with other simulations and experimental results performed by Swillens et al. [14] the unrepaired aneurysm shows both: negative reflections and subsequent pressure drop in the reflected wave. This behaviour can be explained by the augmented capacity of the aneurism sac, and is therefore absent in the normal or repaired aorta simulations.

Another interesting finding is the fact that the Nellix endoprothesis shows an augmented pressure at renal level compared with AFX device. While reflected pressure amplitude at renal level is 45 % the amplitude of the incident pressure wave, this number increases to 60 % for AFX and 79 % increase for Nellix, representing a 33 % and 75 % increase in amplitude ratio compared to normal case, respectively.

Table 1 Simulation parameters. E_{aorta} is the elastic modulus of non-diseased portions of the aorta (E_{nd}), while E_{model} is the elastic modulus of the model-specific portion of the aorta (E_{an} for model 1, Nellix or AFX for models 2 and 3 (E_s), and non-diseased aorta for model 4). *Patient-specific* stands for the diameter vs centreline distance obtained from aortic volume segmentation

Model	E_{aorta}[Pa]	E_{model}[Pa]	h_{aorta}[mm]	h_{model}[mm]	d_{aorta}[mm]	d_{model}[mm]
Aneurysm	4.10^5	6.10^5	2.5	2.0	Patient-specific	Patient-specific
Nellix	4.10^5	200.10^6	2.5	1.0	Patient-specific	10
AFX	4.10^5	5.10^6	2.5	1.0	Patient-specific	25
Normal	4.10^5	4.10^5	2.5	2.5	Patient-specific	25

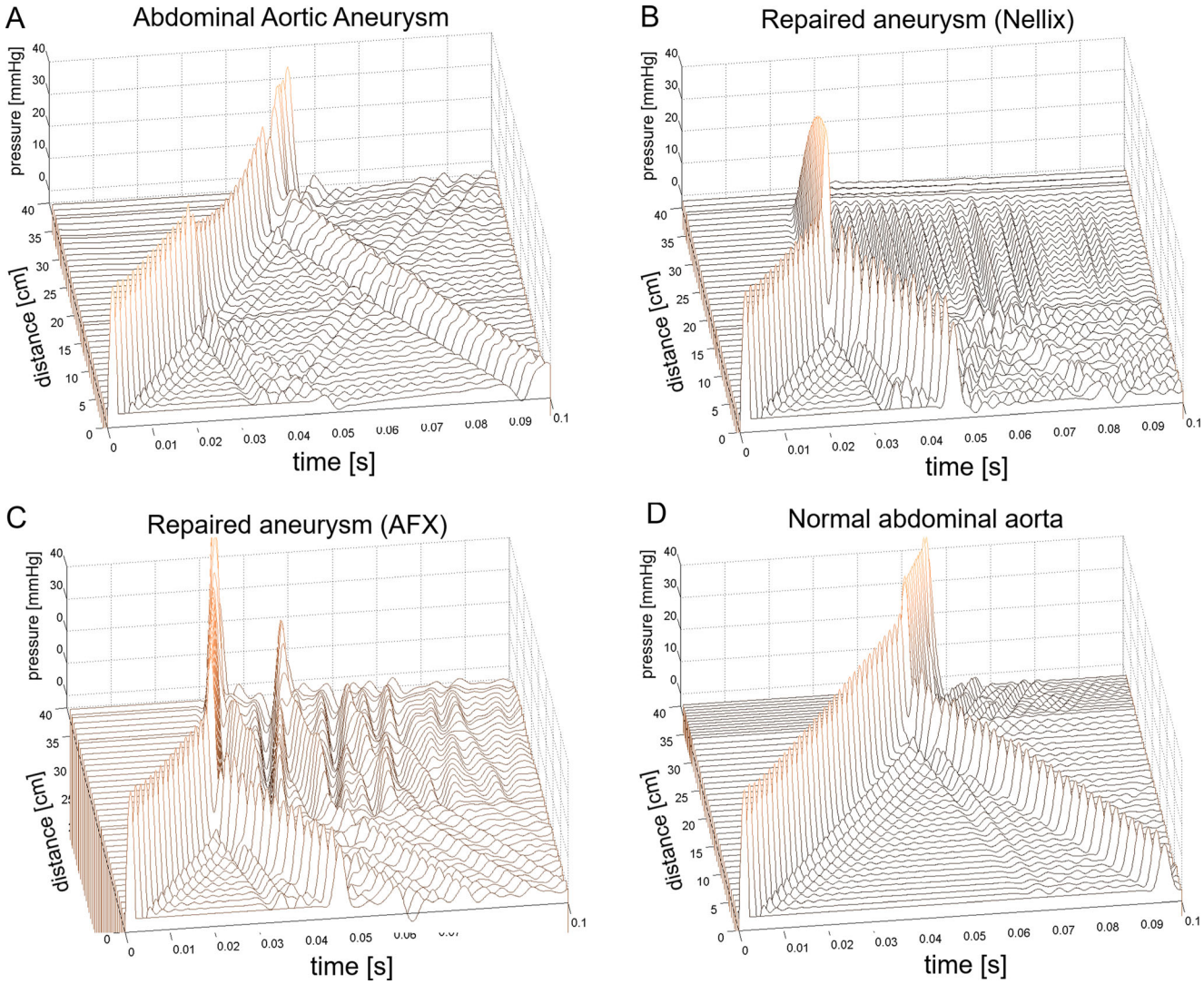

Fig. 3 Pressure waveforms as a function of time and centerline distance. Zero-distance is the model input, while a distance of ~15 cm corresponds to the right renal artery level (refer to Fig. 2 for **a**, **b**, **c** and **d**)

Pressure at renal level is of particular importance due to the baroreceptor function of these organs [24]. Recent studies by Antonello et al. [25] show that there is a continuous decline in renal function after EVAR, regardless of fixation level and independently of pre-existing renal insufficiency. The effects of an augmented blood pressure of mechanical origin due to these novel EVAR devices should be further studied.

Table 2 Amplitude ratio and reflection time (as a fraction of total simulation time) for the different models

	Amplitude ratio (%)		Reflection time [sec] / 0.01 s	
	Input site	Renal level	Input site	Renal level
Bare aneurysm	18	21	0.98	0.55
Repaired (Nellix)	63	79	0.47	0.04
Repaired (AFX)	47	60	0.47	0.04
Normal aorta	35	45	0.95	0.52

Despite the fact that peripheral blood pressure measurements govern cardiovascular treatments, central pressure has been ascribed an increasingly important role in the evaluation of cardiovascular risk [10]. For instance, the central augmentation index provides information on wave reflection patterns, and is a consequence of the early superimposition of the reflected wave onto the forward wave. This parameter provides an indication of the influence of reflected waves on the total pulse pressure. Apart from a high pulse wave velocity, changes in reflection sites can also influence the augmentation index.

This work has limitations that need to be addressed. First, the 1D model considers uniform elasticity and thickness in anterior/posterior/lateral regions of the aneurysm, while it has been demonstrated that aortic

aneurysms are anisotropic both mechanically and geometrically [20]. Also, no variation of thickness or elastic modulus in the cardiac cycle was considered for aortic wall [26], although it is known to vary non-linearly [27]. For instance, the effect of blood pressure on the elastic modulus was not considered, as the patient was under anti-hypertensive treatment and his blood pressure was 50/100 mmHg measured in the brachial artery. Despite these limitations, we can consider that the most interesting findings of this work are related to Nellix and AFX devices, which can be (arguably) considered isotropic in the radial direction, with a nominal constant diameter and Young modulus. Related to this, another limitation arises as no real elastic moduli were assessed for EVAR devices, and an oversimplified mechanical model was used. Nevertheless, we found elastic moduli in the range of simulations conducted by other groups, which obtained values of E = 30 MPa [28] and 8 MPa [29] for a generic abdominal stent graft and a Gore TAG device for aortic arch, respectively. Due to the importance that elastic modulus has on wave propagation and impedance decoupling, real values of this elastic parameter should be obtained experimentally for AFX and Nellix grafts.

Regarding the axisymmetrical nature of the model, it can be difficult to assess a correct diameter versus distance function in highly asymmetrical aneurysm and/or having saccular lesions. Also, when present, blood thrombi are generally non-symmetrical and play an important and complex role on the non-linear mechanical properties of the diseased wall [30]. These non-symmetrical properties should be included in the model in order to obtain more realistic results for such cases.

Additionally, the aortoiliac bifurcation angle was not introduced in the model as the study focused mainly in the characterization of PWF due to EVAR.

5 Conclusion

In this work it was shown that AAA 1D models can be obtained from TC scans, where different patient-specific simulations can be performed. In particular, the effects of different EVAR techniques using Nellix and AFX devices were studied, showing different behaviours in terms of reflected amplitudes and reflection times, especially at renal artery levels. These models could have potential applications in medical EVAR planning, and the validity of the obtained results should be further studied.

Acknowledgments The authors would like to thank Dr. Felipe Gabaldón from the Universidad Politécnica de Madrid, for his kind assistance regarding the use of the 1D flow model.

Compliance with ethical standards

Conflict of interest The authors declare that they have no conflict of interest.

Disclosure statement No potential conflict of interest was reported by the authors.

References

1. Sachs T, Landon B, Pomposelli F, Cotterill P, O'Malley J, Schermerhorn M. Continued expansion of EVAR for intact and ruptured abdominal aortic aneurysm in the Medicare Population, 1995–2008. J Vasc Surg. 2010;52:1115.
2. Diethrich EB. Novel sealing concept in the Endologix AFX unibody stent-graft. J Cardiovasc Surg. 2014;55:93–102.
3. Donayre CE, Zarins CK, Krievins DK, Holden A, Hill A, Calderas C, Velez J, White RA. Initial clinical experience with a sac-anchoring endoprosthesis for aortic aneurysm repair. J Vasc Surg. 2011;53:574–82.
4. Welborn MB 3rd, McDaniel HB, Johnson RC, Kennedy RE, Knott A, Mundinger GH, Stucky FS, Ouriel K. Clinical outcome of an extended proximal seal zone with the AFX endovascular aortic aneurysm system. J Vasc Surg. 2014;60:876–83.
5. Krievins DK, Holden A, Savlovskis J, Calderas C, Donayre CE, Moll FL, Katzen B, Zarins CKEVAR. Using the Nellix sac-anchoring endoprosthesis: treatment of Favourable and adverse anatomy. Eur J Vasc Endovasc Surg. 2011;42:38–46.
6. Karthikesalingam A, Cobb RJ, Khoury A, Choke EC, Sayers RD, Holt PJ, Thompson MM. The morphological applicability of a novel endovascular aneurysm sealing (EVAS) system (Nellix) in patients with abdominal aortic aneurysms. Eur J Vasc Endovasc Surg. 2013;46:440–5.
7. Shaikh U, Chan TY, Oshin O, McWilliams RG, Fisher RK, England A, Torella F. Changes in aortic volumes following endovascular sealing of abdominal aortic aneurysms with the Nellix® endoprosthesis. J Endovasc Ther. 2015;22:881–5.
8. England A, Torella F, Fisher RK, McWilliams RG. Migration of the Nellix endoprosthesis. J Vasc Surg. 2016. doi:10.1016/j.jvs.2016.02.053.
9. Casciaro ME, El-Batti S, Chironi G, Simon A, Mousseaux E, Armentano RL, Alsac JM, Craiem D. Deformable surface model for the evaluation of abdominal aortic aneurysms treated with an endovascular sealing system. Ann Biomed Eng. 2016;44:1381–91.
10. Beckmann M, Jacomella V, Kohler M, Lachat M, Salem A, Amann-Vesti B, Husmann M. Risk stratification of patients with peripheral arterial disease and abdominal aortic aneurysm using aortic augmentation index. PLoS One. 2015. doi:10.1371/journal.pone.0139887.
11. Willemet M, Alastruey J. Arterial pressure and flow wave analysis using time-domain 1-D hemodynamics. Ann Biomed Eng. 2015;43:190–206.
12. Alastruey J, Parker K, Peiró J, Sherwin SJ. Analysing the pattern of pulse waves in arterial networks: a time-domain study. J Eng Math. 2009;64:331–51.
13. Peiro J, Sherwin S, Parker K, Franke V, Formaggia L, Lamponi D, Quarteroni A. Numerical simulation of arterial pulse propagation using one-dimensional models. Advances in computational. Bioengineering. 2003;6:1–36.
14. Swillens A, Lanoye L, De Backer J, Stergiopulos N, Verdonck PR, Vermassen F, Segers P. Effect of an abdominal aortic aneurysm on

wave reflection in the aorta. IEEE Trans Biomed Eng. 2008;55:1602–11.
15. Georgakarakos E, Argyriou C, Georgiadis GS, Lazarides MK. Non-invasive pulse wave analysis in a thrombus-free abdominal aortic aneurysm after implantation of a nitinol aortic endograft. Front Surg. 2016. doi:10.3389/fsurg.2015.00068.
16. Afkari D, Gabaldón F. Fluid-solid interaction in arteries incorporating the autoregulation concept in boundary conditions. Comsput Methods Biomech Biomed Engin. 2016;19:985–1001.
17. Calvo, FJ. Simulación del fluido sanguíneo y su interacción con la pared arterial mediante modelos de elementos finitos [Simulation of blood flow and its interaction with arterial wall using finite element methods] (doctoral thesis). UPM, Madrid. 2006.
18. Länne T, Sonesson B, Bergqvist D, Bengtsson H, Gustafsson D. Diameter and compliance in the male human abdominal aorta: influence of age and aortic aneurysm. Eur J Vasc Surg. 1992;6:178–84.
19. Sonesson B, Hansen F, Stale H, Länne T. Compliance and diameter in the human abdominal aorta: the influence of age and sex. Eur J Vasc Surg. 1993;7:690–7.
20. Thubrikar MJ, Labrosse M, Robicsek F, Al-Soudi J, Fowler B. Mechanical properties of abdominal aortic aneurysm wall. J Med Eng Technol. 2001;25:133–42.
21. Zahora J, Hanus J. Model of mechanical properties of nitinol stent. Proceedings XVII IMEKO World Congress. 2003;13:1757–9.
22. Santos I, Rodrigues A, Figueiredo L, Rocha LA, Tavares JM. Mechanical properties of stent–graft materials. Proceedings of the Institution of Mechanical Engineers, Part L: Journal of Materials: Design and Applications. 2012;226:330–41.
23. Böckler D, Holden A, Thompson M, Hayes P, Krievins D, de Vries JP, Reijnen MM. Multicenter Nellix EndoVascular aneurysm sealing system experience in aneurysm sac sealing. J Vasc Surg. 2015;62:290–8.
24. Kirchheim H, Ehmke H, Persson P. Physiology of the renal baroreceptor mechanism of renin release and its role in congestive heart failure. Am J Cardiol. 1988;62:68E–71E.
25. Antonello M, Menegolo M, Piazza M, Bonfante L, Grego F, Frigatti P. Outcomes of endovascular aneurysm repair on renal function compared with open repair. J Vasc Surg. 2013;58:886–93.
26. Khanafer K, Duprey A, Zainal M, Schlicht M, Williams D, Berguer R. Determination of the elastic modulus of ascending thoracic aortic aneurysm at different ranges of pressure using uniaxial tensile testing. J Thorac Cardiovasc Surg. 2011;142:682–6.
27. Craiem D, Graf S, Salvucci F, Chironi G, Megnien JL, Simon A, Armentano RL. The physiological impact of the nonlinearity of arterial elasticity in the ambulatory arterial stiffness index. Physiol Meas. 2010;31:1037–46.
28. Frauenfelder T, Lotfey M, Boehm T, Wildermuth S. Computational fluid dynamics: hemodynamic changes in abdominal aortic aneurysm after stent-graft implantation. Cardiovasc Intervent Radiol. 2006;29:613–23.
29. Chen D, Müller-Eschner M, Rengier F, Kotelis D, Böckler D, Ventikos Y, Xu Y, Zeng Y, Peng Y, Tengg-Kobligk v, Preliminary Study HA. Of fast virtual stent-graft deployment: application to Stanford type B aortic dissection. Int J Adv Robot Syst. 2013. doi:10.5772/55269.
30. van Dam EA, Dams SD, Gerrit WMP, Rutten MCM, Schurink GWH, Buth J, van de Vosse FN. Non-linear viscoelastic behavior of abdominal aortic aneurysm thrombus. Biomech Model Mechanobiol. 2008;7:127–37.